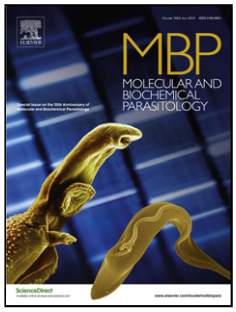

Title: Metformin promotes autophagy in *Echinococcus granulosus* larval stage

Authors: Julia A. Loos, María Celeste Nicolao, Andrea C. Cumino

PII: S0166-6851(18)30083-5
DOI: https://doi.org/10.1016/j.molbiopara.2018.07.003
Reference: MOLBIO 11136

To appear in: *Molecular & Biochemical Parasitology*

Received date: 10-4-2018
Revised date: 21-6-2018
Accepted date: 9-7-2018

Please cite this article as: Loos JA, Nicolao MC, Cumino AC, Metformin promotes autophagy in *Echinococcus granulosus* larval stage, *Molecular and Biochemical Parasitology* (2018), https://doi.org/10.1016/j.molbiopara.2018.07.003

Metformin promotes autophagy in *Echinococcus granulosus* larval stage

Julia A. Loos[a,b], María Celeste Nicolao[a,b] and Andrea C. Cumino[a,b,c]*

[a] *Laboratorio de Zoonosis Parasitarias, Departamento de Biología, Facultad de Ciencias Exactas y Naturales, Universidad Nacional de Mar del Plata (UNMdP), Funes 3350, Nivel Cero, (7600) Mar del Plata, Argentina*

[b] *Consejo Nacional de Investigaciones Científicas y Técnicas (CONICET), Argentina.*

[c] *Departamento de Química, Facultad de Ciencias Exactas y Naturales, Universidad Nacional de Mar del Plata (UNMdP), Funes 3350, Nivel 2, (7600) Mar del Plata, Argentina*

*Corresponding author.

Laboratorio de Zoonosis Parasitarias, Departamento de Biología, Facultad de Ciencias Exactas y Naturales, Universidad Nacional de Mar del Plata (UNMdP), Funes 3350, Nivel Cero, (7600) Mar del Plata, Argentina.

Tel.: +54-223-4752426 ext 450. *E-mail address*: acumino@mdp.edu.ar

Graphical abstract

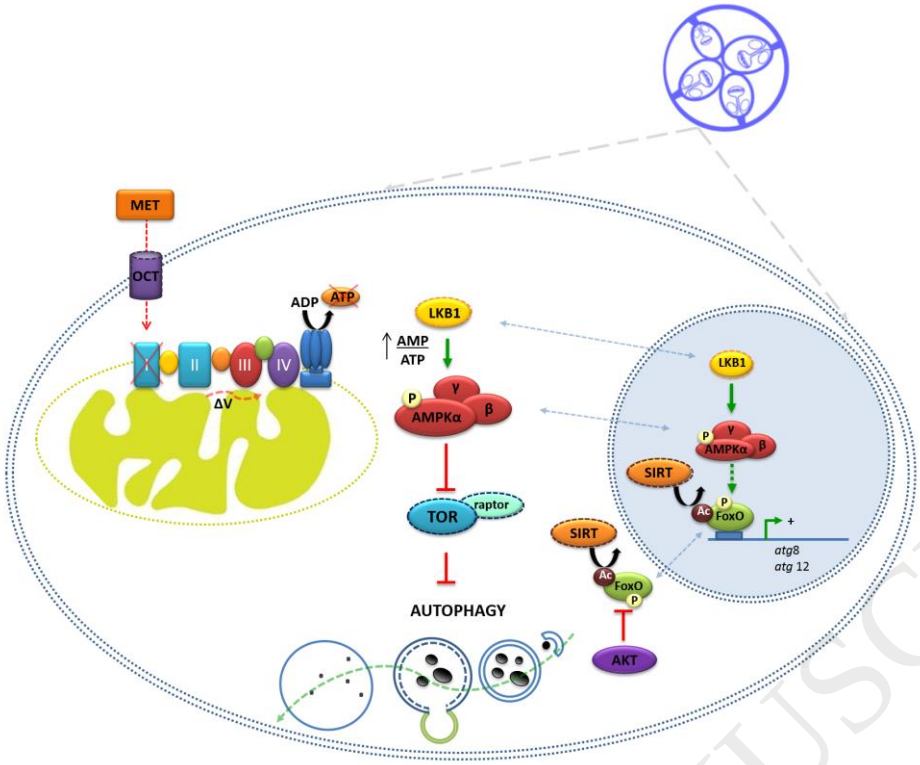

HIGHLIGHTS

- We demonstrate that metformin induces autophagy in *Echinococcus granulosus* – Glycogen-filled vesicles were mobilized in response to metformin – Key Eg-*atg* genes and Eg-*fox*O were overexpressed, suggesting transcriptional regulation. – Metformin activates autophagy through the AMPK-FoxO signaling pathway.

ABSTRACT

Cystic echinococcosis is a neglected parasitic disease caused by the larval stage of *Echinococcus granulosus* for which an effective treatment is not yet available. Since autophagy constitutes a homeostatic mechanism during stress, either inhibition or activation of its activity might be detrimental for survival of the parasite. Amongst the critical molecules that regulate autophagy, TOR, AMPK and sirtuins are the best characterized ones. Previously, we have identified the autophagic machinery, the occurrence of TORC1-controlled events, and the

correlation between autophagy and the activation of the unfolded protein response in *E. granulosus* larval stage. In addition, we have demonstrated that the parasite is susceptible to metformin (Met), a drug that indirectly activates Eg-AMPK and induces energy stress. In this work, we demonstrate that Met induces autophagy in the *E. granulosus* larval stage. Electron microscopy analysis revealed the presence of autophagic structures in Met-treated protoscoleces. In accordance with these findings, the autophagic marker Eg-Atg8 as well as the transcriptional expression of Eg-*atg*6, Eg-*atg*8, Eg-*atg*12 and Eg-*atg*16 genes were significantly up-regulated in Met-treated parasites. The induction of the autophagic process was concomitant with Eg-*fox*O over-expression and its nuclear localization, which could be correlated with the transcriptional regulation of this pathway. On the other hand, the expression of Eg-AKT and Eg-Sirts suggests a possible participation of these conserved proteins in the regulation of Eg-FoxO. Therefore, through pharmacological activation of the AMPK-FoxO signaling pathway, Met could play a role in the death of the parasite contributing to the demonstrated anti-echinococcal effects of this drug. The understanding of the regulatory mechanisms of this pathway in *E. granulosus* represents a solid basis for choosing appropriate targets for new chemotherapeutic agents.

Keywords: Metformin, autophagy, AMPK-FoxO signal pathway, glycophagy

Keywords: *Echinococcus*, autophagy, metformin, AMPK-FoxO signal pathway, glycophagy

1. Introduction

Echinococcus granulosus is the causative agent of cystic echinococcosis, a zoonosis endemic worldwide. Its life cycle involves two mammalian hosts. The intermediate host (usually ungulate species and, accidentally, humans) ingests eggs that develop into a hydatid cyst containing protoscoleces. Infection in the definitive host (dogs or other canids) arises from the ingestion of protoscoleces encysted in intermediate host viscera. In the small intestine, they

develop into adult tapeworms that can reside for long periods. In addition, *E. granulosus* shows an alternative reverse development, in which protoscoleces that are released from a ruptured cyst in an intermediate host are capable of differentiating asexually into secondary hydatid cysts [1].

Echinococcus granulosus, like other parasitic helminths, has to adapt to different environments in which the availability of oxygen and food varies widely [2]. Beyond a certain threshold, such fluctuations in the external conditions are considered stresses, meaning that the organism response to these stresses determines whether it can function properly and survive [3]. During the response to stress, cells undergo rapid changes to protect themselves against potential injury. One of the key pathways that mediate stress-induced metabolic adaptation is autophagy [3].

Autophagy is a catabolic process highly conserved in eukaryotes, in which part of the cytoplasmic content (including damaged organelles and protein aggregates) is sequestered into double-membrane vesicles, degraded by lysosomal activity, and recycled into macromolecules that return to the cytoplasm [4]. A well-orchestrated program including over 30 autophagy-related (Atg) genes controls autophagy, which can be activated by nutrient starvation and subsequent inhibition of mechanistic target of rapamycin (mTOR) signaling or by induction of the unfolded protein response (UPR) as a result of the accumulation of misfolded proteins aggregates [5, 6]. Recently, we have reported the identification of the core autophagic machinery, the occurrence of TORC1 (Target of Rapamycin Complex 1)-controlled events, and the correlation between autophagy and the activation of UPR by bortezomib in *E. granulosus* larval stage [7, 8]. In addition, we have demonstrated that both larval forms of *E. granulosus* are susceptible to metformin (Met), an anti-hyperglycemic drug that indirectly activates Eg-AMPK (AMP-activated protein kinase), as a consequence of cellular energy charge depletion [9, 10]. In conditions where nutrients are scarce, the traditional pathways of autophagy induction are either through AMPK-TOR-ULK1 (unc-51 like autophagy activating kinase) mediated signaling, activated by an increase in the AMP/ATP ratio, or through the AMPK-Sirt1 (sirtuin-1)-FoxO

(Forkhead box transcription factor class O) pathway, activated by increased NAD^+ concentration [11]. However, it remains unknown whether energy depletion induces autophagy in the parasite.

AMPK possesses at least two different ways to release the TORC1-mediated repression on autophagy induction in mammalian cells under energy stress. On the one hand, it phosphorylates and activates TSC2, a negative regulator of TORC1 absent in *Echinococcus* sp.; and on the other, it phosphorylates and inactivates raptor, a subunit of TORC1 [12], whose regulation has not yet been explored in the parasite. Alternatively, AMPK participates in a positive amplification loop with Sirt1 to initiate autophagy under nutritional stress conditions [13]. AMPK and sirtuins (NAD^+-dependent deacetylases) are fuel-sensing molecules that have coexisted in cells throughout evolution. When activated by metabolic stress, AMPK maintains cellular energy homeostasis by switching on catabolic pathways and switching off ATP-consuming processes [14]. Sirtuins, in turn, have many actions but are best known for their role in mediating the increase in longevity caused by caloric restriction in several species [13]. On the other hand, FoxOs represent a subfamily of transcription factors conserved from *Caenorhabditis elegans* (known as DAF-16 -abnormal dauer formation protein 16) to mammals (FoxO1 -FKHR-, FoxO3 -FKHRL1-, FoxO4 –AFX- and FoxO6 [15]) that integrate signals coming from nutrient deprivation and oxidative stress, to coordinate transcriptional activation of genes involved in cellular metabolism and autophagy. They act as potent transcriptional activators of some autophagy genes by binding to the conserved consensus core recognition motif TTGTTTAC [16, 17]. As in other invertebrates, a single Eg-FoxO transcription factor was identified in *E. granulosus*, as well as conserved consensus sequences for FoxO binding in autophagy genes [7]. The regulation of FoxO is achieved by changes at the protein levels, the subcellular localization and the transcriptional activity, which occurs through post-translational modifications, including phosphorylation, acetylation and ubiquitination [18]. Previously, it has been reported that, under glucose deprivation conditions, FoxO factors activate the expression of genes involved in autophagy pathways, such as *gabarapl*1 and *atg*12, in diverse cell types [19, 20].

Here we demonstrate that Met induces autophagy in the larval stage of *E. granulosus* and we discuss possible contribution of Eg-FoxO and sirtuins in this process. However, further studies are needed to shed light on the molecular mechanisms underlying the ability of the drug to regulate this process in the parasite.

2. Materials and methods

2.1. *Ethics statement*

Animal procedures and management protocols were performed according to the National Health Service and Food Quality (SENASA) guidelines, Argentina, and with the 2011 revised form of The Guide for the Care and Use of Laboratory Animals published by the U.S. National Institutes of Health. Experimental protocols were evaluated and approved by the Animal Experimental Committee at the Faculty of Exact and Natural Sciences, Mar del Plata University (permit number: 2555-08-17included into OCA 493/17).

2.2. *In vitro culture of protoscoleces, metacestodes and microcyst obtainment*

Echinococcus granulosus protoscoleces were removed aseptically from hydatid cysts of infected cattle presented for routine slaughter at the Liminal abattoir (official number: 3879) located in the Southeast of Buenos Aires, Argentina. Viable protoscoleces with conserved morphology (n=3,000) were cultured in 24-well culture plates using medium 199 (Gibco) supplemented with glucose (4 mg/ml) and antibiotics (penicillin, streptomycin and gentamicin 100 µg/ml) under normal atmospheric conditions as we previously reported [7]. Additionally, *E. granulosus* murine cysts (n= 10-20) were incubated in Leighton tubes under the same culture conditions as mentioned for protoscoleces [9]. *In vitro* protoscolex treatments were performed with 1, 5 and 10 mM Met and with 10 and 100 µM rapamycin for different periods according to the experiment. Otherwise, *in vitro* metacestode treatments were performed with 10 mM Met for 48 h. For further molecular assays, parasites were washed with sterile and RNAse-free PBS

and maintained at −80 °C until experimental use. Each experiment was performed using three replicates per treatment condition and repeated three times.

Finally, to allow the development of vesicularised protoscoleces and microcysts, protoscoleces were cultured in medium 199 supplemented with antibiotics (penicillin, streptomycin and gentamicin; 100 µg/ml), glucose (4 mg/ml), insulin (1.2 U ml-1) and 15% FBS as we already reported [7]. The complete process was followed every day under an inverted light microscope. Different samples were taken during the pre-microcyst development process which were used for immunohistochemistry assays.

2.3. Estimation of acidic vesicular organelles in metformin-treated protoscoleces.

Presence of acidic vesicular organelles (AVOs) was assessed through vital staining with acridine orange as reported [21]. Briefly, protoscoleces (1 x 10^3) incubated under control conditions or treated with Met (1 and 5 mM) and Rm (10 and 100 µM) during 4 h, were incubated with 1 mg/ml acridine orange (Sigma, USA) in 10 mM HEPES pH 7.4 for 30 min at 4 ºC in darkness. The acridine orange was removed and the fluorescence was registered with a spectrofluorimeter (model F-4500; Hitachi). Dye was excited at 480 nm and the emitted fluorescence was collected using band pass filters: > 600 nm. Each experiment was performed in triplicate and individually corrected for autofluorescence as described [22]. Protoscoleces were also observed using an inverted confocal laser scanning microscope (Nikon, Confocal Microscope C1). Images were analyzed using Image J software (NIH). Red fluorescence of acridine orange images was calculated using NIH Image J software (http://rsb.info.nih.gov/ij/).

2.4. Identification of autophagic structures by transmission electron microscopy

Control and Met-treated protoscoleces (1 mM Met for 4 d) were fixed with 3% glutaraldehyde in sodium cacodylate buffer for 24 h at 4 ºC. Then, the specimens were post-fixed in 2% OsO4 in cacodylate buffer, dehydrated in a graded acetone series, embedded in resin epoxy and finally

examined with a JEM 1200 EX II (JEOL Ltd., Tokio, Japon) transmission electron microscope at 80 Kv.

2.5. Expression analysis of autophagic genes and Eg-*foxO*

Extractions of total RNA from *E. granulosus* protoscoleces and metacestodes, RT-PCR and q-PCR were carried out as described [23]. The levels of gene expression in control and Met-treated parasites were determined by cDNA synthesis using 10 or 5 µg of total RNA from protoscoleces and metacestodes, respectively (with Superscript II reverse transcriptase – Invitrogen, Argentine- and Pfu–Promega, USA- DNA polymerase). The RT-PCR amplification of Eg-*atg*6, Eg-*atg*8, Eg-*atg*12, Eg-*atg*16 and Eg-*foxO* was performed by using previously designed primers [7]. The same primers were used for qPCR amplification, except for the Eg-*atg*6 gene, for which a new set of primers was designed (Eg-*atg*6-f, 5´-GACTCCACTACCTCTCTACAATTCTC -3´ and Eg-*atg*6-r, 5´-GTACTTGAGATCCATCAGAAGCATTTTCAAC -3´), which amplified a fragment of 268 bp. *Echinococcus granulosus* actin I and ezrin-like protein (*act*I, GenBank accession number **L07773**; *elp*, GenBank accession number **CBH50747**) were used as reference genes in RT-PCR and qPCR assays, respectively [9, 24]. The primers designed for Eg-*elp* were Eg-*elp*-f (5´-CTACAGCTGAGTCACAGTTAG-3´) and Eg-*elp*-r (5´- ATCCAATCTTAGAAAGGTTG -3´), whose amplicon size was 158 pb. RT-PCR reactions were performed under the following conditions: 94ºC for 5 min, followed by 30 cycles of 94 °C (30 s), 45 °C (1 min), and 72 °C (1 min) plus a single step at 72 °C for 10 min, while qPCR reactions were conducted under the following conditions: 94ºC for 10 min, followed by 35 cycles of 94 °C (15 s), 55 °C (30 s), and 72 °C (30 s). The relative quantification of mRNA expression was calculated according to the comparative threshold cycle (Ct) method. Each experiment was performed using three replicates per treatment condition and repeated three times.

2.6. Sequences analysis of Echinococcus class III NAD^+-dependent histone/protein deacetylases (sirtuins)

BLASTp searches for sirtuin homologs in the *E. granulosus* genome database (http://www.sanger.ac.uk/Projects/Echinococcus, [25]) were performed using orthologs from *Mus musculus* and *Homo sapiens* as queries. These searches allowed the identification of three putative orthologous genes of class I sirtuins whose predicted open reading frames were analyzed. Orthologs were selected based on reciprocal best BLAST hits [26, 27] on an E-value cut-off of $1e^{-25}$ and on the presence of the characteristic domains in the deduced amino acid sequences. Sequence alignments were generated with the CLUSTALX software program and the modeling of secondary structures of the putative deacetylases was obtained from the deduced primary structures using the Gen-THREADER (http://bioinf.cs.ucl.ac.uk/psipred/psiform.html).

2.7. Western blot analysis and immunohistochemistry

The western blot procedure was performed as previously described [23]. Briefly, the polypeptides were separated by SDS–PAGE on 10% or 15% polyacrylamide gels and electroblotted onto a nitrocellulose membrane (HyBond C; Amersham, Argentina). Then, they were incubated with primary polyclonal antibody directed against the N-terminus of human LC3 (MAP LC3β clone H-50, Santa Cruz sc-28266, USA, 1:1000 dilution), primary polyclonal antibody directed against phosphorylated human FoxO3 (p-FKHRL1 (Ser 253) antibody, Santa Cruz sc-12897, USA, 1:1000 dilution), primary polyclonal antibody directed against acetylated human FoxO1A (Ac-FKHR (D19) antibody, Santa Cruz sc-49437, USA, 1:1000 dilution), or with primary monoclonal antibody of human actin (JLA-20, Developmental Studies Hybridoma Bank-DSHB, USA, 1:2000 dilution) as protein loading control. The anti-LC3β antibody used in these assays is directed against an epitope which showed 52% amino acid identity with the N-terminus of the possible orthologs of *E. granulosus* (Eg-Atg8). On the other hand, the anti-FoxO-P and anti-FoxO-Ac antibodies are directed against a short amino acid sequence

(containing the phosphorylated Ser or acetylated Lys) of Hs-FoxO3 and Hs-FoxO1, respectively, which showed 70% and 50% amino acid identity with the possible ortholog of the parasite (Eg-FoxO). Then, the membranes were incubated with goat anti-rabbit immunoglobulin (Ig)-AP conjugate (catalogue no.170-6518; Bio-Rad). The optical density from each band of interest was normalized to its respective actin density to correct any possible unequal loading.

In parallel, for *in toto* immunohistochemistry, vesicularised protoscoleces (pre-microcysts), microcysts, and control and Met-treated protoscoleces were processed for Eg-Atg8 analysis, as previously described [7]. In addition, the expression and subcellular localization of a phosphorylated (Ser352) and an acetylated (Lys373) form of Eg-FoxO were analyzed in control and Met-treated protoscoleces using the same antibodies as for the Western blots (1/50 dilution). In both cases, the samples were incubated with a secondary antibody conjugated with Alexa 488 fluorescent dye. Green fluorescence intensities in representative nuclear and cytoplasmic areas were quantified to calculate the quotient of nuclear intensity over cytoplasmic intensity using the ImageJ program [28, 29].

Expression of Eg-AKT was also assessed in protoscoleces using a polyclonal antibody directed against total mouse AKT (also known as PKB) (Akt antibody, Cell Signalling cat no. 9272, USA, 1:1000 dilution). The anti-AKT antibody used in these assays is directed against an epitope which showed 80 % amino acid identity with the possible orthologs of *E. granulosus* (Eg-AKT) and *E. multilocularis* (GenBank annotated as **CCW28045** and reported by [30]). Negative controls consisted of omission of primary antibody.

3. Results

3.1. Detection of lysosomal activity and autophagic structures in metformin-treated protoscoleces

In order to estimate the possibility that Met triggers autophagic events in protoscoleces, we performed fluorometric determinations from samples incubated in the presence of acridine

orange. Acridine orange is a pH-sensitive dye that emits red fluorescence in lysosome-like acidic intracellular compartments, which characterize the autophagy. By confocal microscopy, we observed an increase of acidic vesicles in Met-treated parasites compared to the control group (Fig. 1A). Likewise, by fluorometric quantification, we determined an increase in the relative fluorescence levels of Met-treated protoscoleces compared to rapamycin-treated protoscoleces (positive control for induction of autophagy) (Fig. 1B).

Additionally, we carried out TEM analysis of control and pharmacologically treated samples. The tissue ultrastructure in untreated protoscoleces appeared unaltered with glycogen deposits in the tegumental cells (Fig. 1Ca,b). Major effects of Met include the appearance of lysosomes, autophagosomes and autolysosomes (Fig. 1Cc,d). Figs. 1Cc and 1Cd illustrate the presence of autophagosomes containing partially degraded glycogen vesicles. In addition, contraction of the distal cytoplasm was evident after drug treatment (Fig. 1Cc).

3.2. Expression and immunolocalization analysis of Eg-Atg8 in protoscoleces and microcysts

To evaluate the pharmacological induction of autophagy in the larval stage of *E. granulosus*, we performed immunoassays using a rabbit polyclonal antibody directed against the N-terminal of human MAP LC3β. The Eg-Atg8 protein (a LC3β-homolog) was detected as a single band of the expected size (14 kDa) in both control and Met-treated protoscoleces (Fig. 2A). A second band, corresponding to the Eg-Atg8.1 protein conjugated to phosphatidylethanolamine (Eg-Atg8-PE), was detected only in the Met-treated protoscoleces. No band was detected when the strips were incubated with the secondary antibody alone (data not shown). Moreover, by *in toto* immunolocalization assays, we detected Eg-Atg8.1 expression with both diffuse and punctate staining (Fig. 2B). Fluorescent punctate images were often detected in the tegument of control (Fig. 2Ba-d) and Met-treated protoscoleces (Fig. 2Be-h). In turn, Eg-Atg8.1 was observed in the peripheral and central cytoplasm of calcareous corpuscles of Met-treated protoscoleces (Fig. 2Be,f). Finally, in the morphological stages involved in the *in vitro* de-differentiation process of

protoscoleces to microcysts, the fluorescence signal became mainly restricted to the bladder and the number of puncta in the tegument was smaller in relation to the observed in protoscoleces (Supplementary Fig. S1). Non-specific fluorescent signal was detected in the rostellar hooks. The fluorescence pattern was not observed when the parasites were incubated with secondary antibody alone (data not shown).

3.3. Expression analysis of autophagy-related genes in metformin-treated larval stage

Subsequently, we also analyzed the transcriptional expression of the Eg-*atg*6, Eg-*atg*8, Eg-*atg*12 and Eg-*atg*16 genes from protoscoleces and metacestodes. RT-PCR showed a considerable increase in these transcripts in Met-treated parasites in comparison with the control groups (Fig. 3A-C). By qPCR, we found that the transcript levels for Eg-*atg*6, Eg-*atg*8, Eg-*atg*12 and Eg-*atg*16 increased two-, eight-, five- and four-fold in Met-treated protoscoleces and two-, five-, two- and three-fold in Met-treated metacestodes, respectively, relative to the controls (Fig. 3B-D).

3.4. Expression and immunolocalization analysis of Eg-FoxO in metformin-treated protoscoleces

We have previously identified and analyzed the expression of a gene encoding FoxO in *E. granulosus* [7]. Here, both by RT-PCR and qPCR analysis, we found that Met induced an increase in the transcriptional expression of Eg-*fox*O (three-fold) in protoscoleces (Fig. 4A,B). We extended the study and demonstrated that the Eg-FoxO sequence conserves post-translationally modifiable residues, such as one phosphorylable serine residue and one acetylable lysine residue (Fig 4D). Subsequently, by immunoassays, we detected the expression of a phosphorylated (Ser352, corresponding to the human Ser253) and an acetylated (Lys373, corresponding to the human Lys274) form of Eg-FoxO in control and Met-treated protoscoleces (Fig. 4C). In both cases, a single band of the expected size (approximately 85 kDa) and similar intensity was reveled in the two samples (Fig. 4C). No band was detected when the strips were

incubated with the secondary antibody alone (data not shown). Then, by *in toto* immunolocalization assays, we detected the expression and subcellular localization of Eg-FoxO-P and Eg-FoxO-Ac in control and Met-treated protoscoleces (Fig. 4E, F). Interestingly, similar expression patterns were observed in both samples. Expression of Eg-FoxO-P was only detected in the cytoplasm, mainly in tegumental cells (Fig. 4Ei-p). In contrast, Eg-FoxO-Ac was observed in both the nucleus and the cytoplasm of the cells of control and Met-treated samples, although in Met-treated protoscoleces the nuclear expression was higher than in the control condition (Fig. 4Ea-h and 4F). The fluorescence pattern was not observed when the parasites were incubated with the secondary antibody alone (data not shown).

3.5 Occurrence and expression of key genes possibly involved in the regulation of Eg-FoxO

After identifying a phosphorylated and an acetylated form of Eg-FoxO, we analyzed the occurrence and expression of Eg-AKT kinase and class III deacetylases (Eg-Sirts) in the larval stage of *Echinococcus* because they may be involved in the post-translational regulation of this transcription factor. By *in toto* immunolocalization assays from protoscoleces, the expression of total Eg-AKT was detected in the tegument and surrounding the nuclei (Supplementary Fig. S2A). Additionally, three orthologs to human Sirt1, Sirt2 and Sirt3 deacetylases showed to be constitutively expressed in *E. granulosus* larval stage (Supplementary Fig. S2B). Eg-Sirt1-3 contain in their structures a conserved catalytic core domain which is composed of a NAD^+-binding Rossmann fold domain and a smaller Zn^{2+}-binding domain that contains four highly conserved Cys residues (Supplementary Fig. S2C). Based on sequence homology with human orthologs, Eg-Sirt1, Eg-Sirt2, and Eg-Sirt3 belong to class I sirtuins and they should exhibit deacetylase activity.

4. Discussion

Cellular stress provoked by external or internal signals activates certain integrated processes liable of restoring cell homeostasis or inducing cellular death. Fundamental pathways that constitute integral parts of this response include the autophagy, UPR, hypoxic signaling, and mitochondrial biogenesis [31]. Among the critical molecules that regulate autophagy, TOR and AMPK have been best characterized, and more recent roles for the sirtuins have been described [3]. While TOR activity depends on diverse positive signals (such as high energy levels, the presence of growth factors or amino acids) which result in the inhibition of autophagy, AMPK is activated under low energy conditions, leading to autophagy induction [12]. Previously, we showed that the TORC1-inhibitor, rapamycin, is able to induce autophagy in *Echinococcus* even under nutrient-rich conditions [7]. On the other hand, we described the indirect Eg-AMPK activation in response to Met-treatment in the larval stage of the cestode [9]. Therefore, based on reports that indicate that Met induces autophagy through AMPK activation [32, 33], the aim of our study was to assess whether Met induces the autophagy machinery and whether the regulation involves Eg-FoxO activation in the parasite.

At the cellular level, TEM micrographs showed the presence of morphological indicators of the different stages of the autophagic process in *Echinococcus* (Fig. 1C). We observed that Met treatment significantly increased the numbers of autophagosomes and autolysosomes in protoscoleces (Fig. 1Cc,d). In addition, the detection of autophagosomes in control protoscoleces (Fig. 1Ca,b) was indicative of the basal participation of this process in the physiology of the parasite. Considering that the autolysosome is an acidic compartment that derives from the fusion of autophagosomes with lysosomes, acidic vesicles detection has been proposed as a late marker of autophagy [34]. Complementarily, experiments performed with acridine orange showed an increase in the content of acidic vesicular organelles in rapamycin- and Met-treated protoscoleces (Fig. 1A,B). Also, in Met-treated parasites, a decrease in the electron-dense glycogen content included in double-membrane vesicles was observed by TEM (Fig. 1Cc,d) suggesting glycophagy occurrence, as it has been described in other invertebrates

[35]. The same glycogen-laden structures were observed in non-treated parasites (Fig. 1 Ca,b), indicating that glycogen autophagy can also occur in basal conditions.

Following, we also confirmed that an increased protein level of Eg-AMPK-P due to Met treatment [9] was accompanied by an increase in Eg-Atg8-PE levels, an indicator of autophagy induction (Fig. 2). In addition, Eg-Atg8 was detected as a punctate pattern in the syncytial tegument and in several parenchymal cells of the soma of protoscoleces. The signal was higher in protoscoleces treated with Met, however, control results again account for the basal autophagic activity in the larval stage. Likewise, high levels of the Eg-Atg8 polypeptide were observed within the free cytoplasmic matrix of the calcareous corpuscles. This agrees with the theory proposed by McCullough and Fairweather [36] regarding the autophagic development of calcareous corpuscles. In this case, the Eg-Atg8 expression was higher in Met-treated parasites than in control, suggesting catabolic induction in these mineralized cells upon pharmacological treatment (Fig. 2B e-f). On the other hand, it has been reported that autophagy also can be rapidly upregulated when the organism is undergoing architectural remodeling [37, 38]. Interestingly, expression of Eg-Atg8 (Supplementary Fig. S1) and Eg-AMPKα [9] was observed in the developmental structures during the de-differentiation process from protoscoleces to microcysts, indicating that both proteins are expressed during the asexual development of *E. granulosus*. These results could account for the anti-echinococcal effects that Met has shown on cyst development [10], and allow the consideration of this drug as a pharmacological alternative during the development of secondary hydatidosis through activation of the AMPK-TORC1-autophagy pathway.

In line with the above findings, the transcriptional expression of Eg-*atg*6, Eg- *atg*8, Eg-*atg*12 and Eg-*atg*16 was found to be increased in both protoscoleces and metacestodes exposed to Met (Fig. 3). This increase in mRNA levels of autophagic genes strengthens the evidence of autophagy induction in presence of Met in agreement with previous reports [39, 40]. In connection with this, it has been proposed that the prolonged induction of the expression of *atg*

genes allows the replenishment of structural autophagic proteins that are destroyed during the autophagosome fusion with the lysosome [41].

Regarding the underlying transcriptional machinery, it has been described that FoxO proteins affect the expression of genes involved in autophagy from flies to mammals, allowing the adaptation of the tissues to the nutrient limitation [42-44]. In fact, FoxO has been reported as necessary and sufficient to induce autophagy in *Drosophila* [45]. Particularly in mammalian cells, FoxO1 and FoxO3 directly bind to the promoters and induce the transcription of genes such as *LC3*B, *gabarapl*1 and *atg*12 [19, 46]. In this work, we detected that Met induces Eg-*fox*O gene expression and that this could stimulate autophagy induction (Fig. 4A,B). These results are consistent with a previous report using MCF-7 breast cancer cells [47], as well as with the increased *foxO*1 mRNA levels detected in the endometrial tissue of PCOS patients treated with Met [48]. Since the Eg-*agt*8 and Eg-*atg1*2 genes possess conserved consensus sequences for the binding of the FoxO transcription factor in the upstream region of their translation initiation codons, it has been considered that they are possible targets of Eg-FoxO [7].

The nuclear localization of FoxO, which is dependent on its phosphorylation and acetylation status, is a prerequisite for its transcriptional function [49, 50]. It is known that FoxO is subject to phosphorylation by AKT, which leads to its nuclear exclusion in presence of growth factors [15, 18, 51]. Here, we identified a conserved phosphorylation site of Eg-FoxO (Ser352, which correspond to Ser253 in Hs-FoxO3) and confirmed the expression of the phosphorylated form of this protein (Eg-FoxO-P352) in the cytoplasm of control and Met-treated protoscoleces (Figs. 4C, D and 4Ei-p), suggesting its possible regulation by AKT. Simultaneously, we demonstrated the Eg-AKT expression (Supplementary Fig. S2A), which in a previous report has been studied as a common mediator of cell signaling pathways initiated by insulin in *E. multilocularis* [30]. On the other hand, the acetylation status of FoxOs, as well as Atg5, Atg7, Atg8 and Atg12, is generally balanced by histone acetylases and sirtuins [52]. Sirt1 is localized primarily in the nucleus and linked to the induction of autophagy through

deacetylation of these proteins [53-55], whereas Sirt2 is found primarily in the cytosol and is the main deacetylase of cytosolic FoxO1 [3, 53, 56]. Firstly, we identified conserved acetylation sites of Eg-FoxO (Lys373, which correspond to Lys274 in Hs-FoxO1), Eg-Atg5 (Lys165, which correspond to Lys130 in Hs-Atg5), and Eg-Atg8.2 (Lys46 and Lys48, which correspond to Lys49 and Lys51 in Hs-FoxO1) as being possible functional sites for Eg-Sirts [25, 50, 57-60]. Then, we confirmed the occurrence and expression of genes encoding *E. granulosus* class I sirtuins (Supplementary Fig. S2 B,C). Particularly, Eg-Sirt1, Eg-Sirt2 and Eg-Sirt3 are expressed in control conditions and their predicted sequences show the presence of catalytic domains conserved in sirtuin family deacetylases, as occurs in other helminths (Supplementary Fig. S2B,C, [59]). Our results showed that the genes encoding Eg-Sirt1 and Eg-Sirt2 have a high expression level in both larval forms, and that the gene encoding Eg-Sirt3 has a low expression level in protoscoleces when compared with metacestodes (Supplementary Fig S2-B), in concordance with Tsai et al [25]. Finally, we detected Eg-FoxO-Ac in both the nucleus and the cytoplasm of control and Met-treated protoscoleces, being the nucleus/cytoplasm ratio higher in pharmacologically treated parasites (Fig. 4Ea-h and 4F). This could explain the transcriptional activation of FoxO-dependent autophagy genes under the drug effect. Moreover, transcription-independent roles have been demonstrated for FoxOs during their cytosol localization [49, 50]. By this way, cytosolic Eg-FoxO-Ac could interact with Eg-Atg7 to induce the autophagic process, as has been reported for other systems [50].

Currently, the therapeutical targeting of FoxO signaling pathways is being proposed as a strategy for the development of efficacious agents for certain diseases including some cancers [60]. Based on this and the fact that *Echinococcus* possess a single FoxO transcription factor, the study of its target genes as well as the analysis of its role in the AMPK/Sirt1/FoxO pathway and in the parasite metabolism will be of interest for its possible interference with therapeutic purposes. Additionally, since FoxO can be a substrate for AMPK [18], it will also be interesting to analyze the possible phosphorylation of Eg-FoxO in Thr278, Ser509, Ser522, Ser681, Ser714

and Ser754 (which correspond to Thr179, Ser399, Ser413; Ser555, Ser588 and Ser626 in Eg-FoxO3) in presence of Met.

AMPK and Sirt1 have similar effects on processes such as cellular fuel metabolism and mitochondrial function. Likewise, both proteins are involved in a positive amplification loop, named Sirt1/AMPK cycle, which acts to initiate autophagy in nutrient deprivation conditions [13]. In our assays, the treatment of *E. granulosus* larval stage with Met promoted catabolic processes such as glycogenolysis, homolactic fermentation and autophagy ([9] and this work). Since Met is well-established to activate both AMPK and Sirt1 [11, 62], it will be of interest in future studies to evaluate the effect of the drug on the activation status of Eg-Sirts in the cestode. Of the seven types of sirtuins (Sirt1-7) present in metazoans, *Echinococcus* spp. express Sirt1-3 and Sirt5-7, but lack Sirt4 in accordance with that reported by Zheng et al., [57]. Considering this and the recent evidence that Sirt 6 induces autophagy via attenuation of AKT signaling [63], it will also be interesting to assess the putative role of these conserved proteins in Eg-FoxO deacetylation as well as in autophagy induction by Met.

Recently, our research group demonstrated that, under both *in vitro* and *in vivo* conditions, the *E. granulosus* larval stage is susceptible to Met [10]. Moreover, here we demonstrated that the drug induces autophagy in the parasite. In our *in vitro* assays, Met concentrations employed were a magnitude of order higher than plasma levels reached on *in vivo* experimental models because, under elevated-glucose conditions, high concentrations of the drug are required to affect the parasite energy-generating systems [9, 10]. Therefore, the above-mentioned further experiments should be carried out using physiological glucose concentrations, under which higher parasite sensitivity to lower drug concentrations is expected.

Although autophagy is a predominantly homeostatic mechanism, it can also play a role in cell death [31]. Therefore, excessive autophagy induced in constant presence of Met, might cause uncontrollable degradation or sequestration of cells contents into autophagosomes resulting in cell death if not properly regulated [64]. Although the role of autophagy in *Echinococcus* remains to be established, the possibility that the parasite benefits from autophagy

as a process that serves to maintain homeostasis is intriguing and merits further studies. From a therapeutic perspective, it will be of great importance to understand how the autophagy could be pharmacologically manipulated to favor prodeath signaling in the parasite.

Acknowledgments

The authors gratefully acknowledge to Dr. J. P. Parody and Dra. M. C. Carrillo (IFISE-CONICET, Facultad de Ciencias Bioquímicas y Farmacéuticas, Universidad Nacional de Rosario, Argentina) for the provision of FoxO antibodies, Lic. D. Villamonte, Lic. V. Daniel, Dra. M.V. Martin (CONICET, Universidad Nacional de Mar del Plata, Argentina), Dra. S. Jurado and R.V. Peralta (Servicio Central de Microscopía Electrónica de la Facultad de Ciencias Veterinarias, Universidad Nacional de La Plata, Argentina) for the technical assistance with confocal and transmission electronic microscopy, respectively, and Dr. S. G. González and Dra. A. Goya (SENASA, Argentina). We also thank the use of facilities at the INBIOTEC-CONICET-FIBA and at the IIB-CONICET-UNMdP, Mar del Plata, Argentina. The *E. multilocularis* and *E. granulosus* genome sequences data mentioned was produced by the Pathogen Sequencing Group of the Wellcome Trust Sanger Institute (Program of Helminth Sequencing; project manager: Dr. Matt Berriman). This work was supported by CONICET (PIP 2015 N°11220150100406) and Universidad Nacional de Mar del Plata (Grant EXA 760/16 and EXA761/16), Argentina.

References

1. Thompson, R.C.A., 1995. Biology and systematics of Echinococcus. In: Thompson R.C.A., Lymbery A, editors. Echinococcus and hydatid disease. Wallingford: CAB International. pp. 1-50.

2. Tielens, A.G.M., 1994. Energy generation in parasitic helminths. Parasitology today. 10, 346-352.

3. Kroemer, G., Mariño, G., Levine, B., 2010. Autophagy and the integrated stress response. Mol Cell. 40, 280-293.

4. Xie, Z., Klionsky, D.J., 2007. Autophagosome formation: core machinery and adaptations. Nat Cell Biol. 9, 1102-1109.

5. Mizushima, N., Komatsu, M., 2011. Autophagy: renovation of cells and tissues. Cell. 147, 728-741.

6. Deegan, S., Saveljeva, S., Gorman, A.M., Samali, A., 2013. Stress-induced self-cannibalism: on the regulation of autophagy by endoplasmic reticulum stress. Cell Mol Life Sci. 70, 2425-2441.

7. Loos, J.A., Caparros, P.A., Nicolao, M.C., Denegri, G.M., Cumino, A.C., 2014. Identification and pharmacological induction of autophagy in the larval stages of *Echinococcus granulosus*: an active catabolic process in calcareous corpuscles. Int J Parasitol. 44, 415-427.

8. Nicolao, M.C., Loos, J.A., Rodrigues, C.R., Beas, V., Cumino, A.C., 2017. Bortezomib initiates endoplasmic reticulum stress, elicits autophagy and death in *Echinococcus granulosus* larval stage. PloS one. 12, e0181528.

9. Loos, J.A., Cumino, A.C., 2015. *In vitro* anti-echinococcal and metabolic effects of metformin involve activation of AMP-activated protein kinase in larval stages of *Echinococcus granulosus*. PloS one. 10, e0126009.

10. Loos, J.A., Dávila, V.A., Rodrígues, C.R., Petrigh, R., Zoppi, J.A., Crocenzi, F.A., Cumino, A.C., 2017. Metformin exhibits preventive and therapeutic efficacy against experimental cystic echinococcosis. PLoS Negl Trop Dis. 11, e0005370.

11. Song, Y.M., Lee, Y.H., Kim, J.W., Ham, D.S., Kang, E.S., Cha, B.S., Lee, H.C., Lee, B.W., 2015. Metformin alleviates hepatosteatosis by restoring SIRT1-mediated autophagy induction via an AMP-activated protein kinase-independent pathway. Autophagy. 11, 46-59.

12. Alers, S., Löffler, A.S., Wesselborg, S., Stork, B., 2012. Role of AMPK-mTOR-Ulk1/2 in the regulation of autophagy: cross talk, shortcuts, and feedbacks. Mol Cell Biol. 32, 2-11.

13. Ruderman, N.B., Xu, X.J., Nelson, L., Cacicedo, J.M., Saha, A.K., Lan, F., Ido, Y., 2010. AMPK and SIRT1: a long-standing partnership?. Am J Physiol Endocrinol Metabol. 298, E751-E760.

14. Hardie, D.G., 2015. AMPK: positive and negative regulation, and its role in whole-body energy homeostasis. Curr Opin Cell Biol. 33, 1-7.

15. Martins, R., Lithgow, G.J., Link, W., 2016. Long live FOXO: unraveling the role of FOXO proteins in aging and longevity. Aging Cell. 15, 196-207.

16. Furuyama, T., Nakazawa, T., Nakano, I., Mori, N., 2000. Identification of the differential distribution patterns of mRNAs and consensus binding sequences for mouse DAF-16 homologues. Biochem J. 349, 629-634.

17. Xuan, Z., Zhang, M.Q., 2005. From worm to human: bioinformatics approaches to identify FOXO target genes. Mech Ageing Dev. 126, 209-215.

18. Calnan, D.R., Brunet, A., 2008. The foxo code. Oncogene. 27, 2276.

19. Ouyang, L., Shi, Z., Zhao, S., Wang, F.T., Zhou, T.T., Liu, B., Bao, J.K., 2012. Programmed cell death pathways in cancer: a review of apoptosis, autophagy and programmed necrosis. Cell Prolif. 45, 487-498.

20. Webb, A.E., Brunet, A., 2014. FOXO transcription factors: key regulators of cellular quality control. Trends in biochemical sciences, 39(4), 159-169.

21. Kanzawa, T., Kondo, Y., Ito, H., Kondo, S., Germano, I., 2003. Induction of autophagic cell death in malignant glioma cells by arsenic trioxide. Cancer Res. 63, 2103-2108.

22. Cumino, A.C., Elissondo, M.C., Denegri. G.M., 2009. Flubendazole interferes with a wide spectrum of cell homeostatic mechanisms in *Echinococcus granulosus* protoscoleces. Parasitol Int. 58, 270-277.

23. Cumino, A.C., Lamenza, P., Denegri, G.M., 2010. Identification of functional FKB protein in *Echinococcus granulosus*: Its involvement in the protoscolicidal action of rapamycin derivates and in calcium homeostasis. Int J Parasitol. 40, 651-661.

24. Espínola, S.M., Ferreira, H.B., Zaha, A., 2014. Validation of suitable reference genes for expression normalization in *Echinococcus* spp. larval stages. PLoS One. 9(7), e102228.

25. Tsai, I.J., Zarowiecki, M., Holroyd, N., Garciarrubio, A., Sanchez-Flores, A., Brooks, K.L., Tracey, A., Bobes, R.J., Fragoso, G., Sciutto, E., Aslett, M., Beasley, H., Bennett, H.M., Cai, J., Camicia, F., Clark, R., Cucher, M., De Silva, N., Day, T.A., Deplazes, P., Estrada, K., Fernández, C., Holland, P.W., Hou, J., Hu, S., Huckvale, T., Hung, S.S., Kamenetzky, L., Keane, J.A., Kiss, F., Koziol, U., Lambert, O., Liu, K., Luo, X., Luo, Y., Macchiaroli, N., Nichol, S., Paps, J., Parkinson, J., Pouchkina-Stantcheva, N., Riddiford, N., Rosenzvit, M., Salinas, G., Wasmuth, J.D., Zamanian, M., Zheng, Y.The Taenia solium Genome Consortium, Cai, X., Soberón, X., Olson, P.D., Laclette, J.P., Brehm, K., Berriman, M., 2013. The genomes of four tapeworm species reveal adaptations to parasitism. Nature. 496, 57-63.

26. Doolittle RF., 1995. The multiplicity of domains in proteins. Ann. Rev. Biochem. 64, 287-314.

27. Tatusov, R.L., Koonin, E.V., Lipman, D.J., 1997. A genomic perspective on protein families. Science. 278, 631-637.

28. Rasband, W.S., 1997-2006. ImageJ, U.S. National Institutes of Health, Bethesda. Maryland, USA, http://rsb.info.nih. gov/ij/.

29. Abramoff, M.D., Magalhaes, P.J., Ram, S.J., 2004. Image Processing with ImageJ. J. Biophotonics. 11, 36-42.

30. Hemer, S., Konrad, C., Spiliotis, M., Koziol, U., Schaack, D., Förster, S., Gelmedin, V., Stadelmann, B., Dandekar, T., Hemphill, A., Brehm, K., 2014. Host insulin stimulates *Echinococcus multilocularis* insulin signalling pathways and larval development. BMC biology. 12, 5.

31. Senft, D., Ronai., 2015. UPR, autophagy, and mitochondria crosstalk underlies the ER stress response. Trends in biochemical sciences. 40, 141-148.

32. Tomic, T., Botton, T., Cerezo, M., Robert, G., Luciano, F., Puissant, A., Gounon, P., Allegra, M., Bertolloto, C., Bereder, J.M., Tartare-Deckert, S., Bahadoran, P., Auberger, P, Ballotti, R., Rocchi, S., 2011. Metformin inhibits melanoma development through autophagy and apoptosis mechanisms. Cell Death Dis. 2, e199.

33. Shi, W.Y., Xiao, D., Wang, L., Dong, L.H., Yan, Z.X., Shen, Z.X., Chen, S.J., Chen, Y., Zhao, W.L., 2012. Therapeutic metformin/AMPK activation blocked lymphoma cell growth via inhibition of mTOR pathway and induction of autophagy. Cell Death Dis. 3, e275.

34. Tettamanti, G., Malagoli, D., 2008. *In vitro* methods to monitor autophagy in Lepidoptera. Methods Enzymol. 451, 685-709.

35. Zirin, J., Nieuwenhuis, J., Perrimon, N., 2013. Role of autophagy in glycogen breakdown and its relevance to chloroquine myopathy. PLoS biology. 11, e1001708.

36. McCullough, J.S., Fairweather, I., 1987. The structure, composition, formation and possible functions of calcareous corpuscles in *Trilocularia acanthiaevulgaris* Olsson 1867 (Cestoda, Tetraphyllidea). Parasitol. Res. 74, 175-182.

37. Tettamanti, G., Saló, E., González-Estévez, C., Felix, D.A., Grimaldi, A., de Eguileor, M., 2008. Autophagy in invertebrates: insights into development, regeneration and body remodeling. Curr Pharm Des. 14, 116-125.

38. González-Estévez, C., Saló, E., 2010. Autophagy and apoptosis in planarians. Apoptosis. 15, 279-292.

39. Kouroku, Y., Fujita, E., Tanida, I., Ueno, T., Isoai, A., Kumagai, H., Ogawa, S., Kaufman, R.J., Kominami, E., Momoi, T., 2007. ER stress (PERK/eIF2α phosphorylation) mediates the polyglutamine-induced LC3 conversion, an essential step for autophagy formation. Cell Death Differ. 14, 230-239.

40. Goussetis, D.J., Altman, J.K., Glaser, H., McNeer, J.L., Tallman, M.S., Platanias, L.C., 2010. Autophagy is a critical mechanism for the induction of the antileukemic effects of arsenic trioxide. J Biol Chem. 285, 29989-29997.

41. Sandri, M., 2010. Autophagy in health and disease. 3. Involvement of autophagy in muscle atrophy. Am J Physiol Cell Physiol. 298, C1291-C1297.

42. Zhao, J., Brault, J.J., Schild, A., Cao, P., Sandri, M., Schiaffino, S., Lecker, S.H., Goldberg, A. L., 2007. FoxO3 coordinately activates protein degradation by the autophagic/lysosomal and proteasomal pathways in atrophying muscle cells. Cell Metab. 6, 472-483.

43. Sengupta, A., Molkentin, J.D., Yutzey, K.E., 2009. FoxO transcription factors promote autophagy in cardiomyocytes. J Biol Chem. 284, 28319–28331.

44. Demontis, F., Perrimon, N., 2010. FOXO/4E-BP signaling in *Drosophila* muscles regulates organism-wide proteostasis during aging. Cell. 143, 813-825.

45. Juhász, G., Puskás, L.G., Komonyi, O., Érdi, B., Maróy, P., Neufeld, T.P., Sass, M., 2007. Gene expression profiling identifies FKBP39 as an inhibitor of autophagy in larval *Drosophila* fat body. Cell Death Differ. 14, 1181-1190.

46. He, C., Klionsky, D.J., 2009. Regulation mechanisms and signaling pathways of autophagy. Annu Rev Genet. 43, 67–93.

47. Queiroz, E.A., Puukila, S., Eichler, R., Sampaio, S.C., Forsyth, H.L., Lees, S.J., Barbosa, A.M., Dekker, R.F., Fortes, Z.B., Khaper, N., 2014. Metformin induces apoptosis and cell cycle arrest mediated by oxidative stress, AMPK and FOXO3a in MCF-7 breast cancer cells. PloS one, 9(5), e98207.

48. Sumarac-Dumanovic, M., Apostolovic, M., Janjetovic, K., Jeremic, D., Popadic, D., Ljubic, A., Micic, J., Dukanac-Stamenkovic, J., Tubic, A., Stevanovic, D., Micic, D., Trajkovic, V., 2017. Downregulation of autophagy gene expression in endometria from women with polycystic ovary syndrome. Mol Cell Endocrinol. 440,116-124.

49. Liu, P., Li, S., Gan, L., Kao, T.P., Huang, H., 2008. A transcription-independent function of FOXO1 in inhibition of androgen-independent activation of the androgen receptor in prostate cancer cells. Cancer Res. 68, 10290-10299.

50. Zhao, Y., Yang, J., Liao, W., Liu, X., Zhang, H., Wang, S., Wang, D., Feng, J., Yu, L., Zhu, W.G., 2010. Cytosolic FoxO1 is essential for the induction of autophagy and tumour suppressor activity. Nat Cell Biol. 12, 665–675.

51. Kalaany, N.Y., Sabatini, D.M., 2009. Tumours with PI3K activation are resistant to dietary restriction. Nature. 458, 725-731.

52. Ng, F., Tang, B.L., 2013. Sirtuins' modulation of autophagy. J Cell Physiol. 228, 2262-2270.

53. Lee, I.H., Cao, L., Mostoslavsky, R., Lombard, D.B., Liu, J., Bruns, N.E., Tsokos, M., Alt, F.W., Finkel, T., 2008. A role for the NAD-dependent deacetylase Sirt1 in the regulation of autophagy. Proc Natl Acad Sci USA. 105, 3374-3379.

54. Hariharan, N., Maejima, Y., Nakae, J., Parik, J., Depinho, R.A., Sadoshima, J., 2010. Deacetylation of FoxO by Sirt1 Plays an Essential Role in Mediating Starvation-Induced Autophagy in Cardiac Myocytes. Circ Res. 107, 1470-1482.

55. Huang, R., Xu, Y., Wan, W., Shou, X., Qian, J., You, Z., Liu, B., Chang, C., Zhou, T., Lippincott-Schwartz, J., Liu, W., 2015. Deacetylation of nuclear LC3 drives autophagy initiation under starvation. Mol Cell. 57, 456-466.

56. North, B.J., Marshall, B.L., Borra, M.T., Denu, J.M., Verdin, E., 2003. The human Sir2 ortholog, SIRT2, is an NAD+-dependent tubulin deacetylase. Mol Cell. 11, 437-444.

57. Zheng, H., Zhang, W., Zhang, L., Zhang, Z., Li, J., Lu, G., Zhu, Y., Wang, Y., Huang, Y., Liu, J., Kang, H., Chen, J., Wang, L., Chen, A., Yu, S., Gao, Z., Jin, L., Gu, W., Wang, Z., Zhao, L., Shi, B., Wen, H., Lin, R., Jones, M.K., Brejova, B., Vinar, T., Zhao, G., McManus, D.P., Chen, Z., Zhou, Y., Wang, S., 2013. The genome of the hydatid tapeworm *Echinococcus granulosus*. Nat Genet. 45, 1168-1175.

58. Iyer, S., Han, L., Bartell, S.M., Kim, H.N., Gubrij, I., de Cabo, R., O'Brien C.A., Manolagas, S.C., Almeida, M., 2014. Sirtuin1 (Sirt1) promotes cortical bone formation by preventing β-catenin sequestration by FoxO transcription factors in osteoblast progenitors. J Biol Chem. 289 (35), 24069-24078.

59. Lancelot, J., Cabezas-Cruz, A., Caby, S., Marek, M., Schultz, J., Romier, C., Sippl, W., Jung, M., Pierce, R.J., 2015. Schistosome sirtuins as drug targets. Future Med Chem. 7, 765-782.

60. Klotz, L.O., Sánchez-Ramos, C., Prieto-Arroyo, I., Urbánek, P., Steinbrenner, H., Monsalve, M., 2015. Redox regulation of FoxO transcription factors. Redox Biol. 6:51-72.

61. Farhan, M., Wang, H., Gaur, U., Little, P.J., Xu, J., Zheng, W., 2017. FOXO Signaling Pathways as Therapeutic Targets in Cancer. Int J Biol Sci. 13, 815-827.

62. Caton, P.W., Nayuni, N.K., Kieswich, J., Khan, N.Q., Yaqoob, M.M., Corder, R., 2010. Metformin suppresses hepatic gluconeogenesis through induction of SIRT1 and GCN5. J Endocrinol. 205, 97-106.

63. Shao, J., Yang, X., Liu, T., Zhang, T., Xie, Q.R., Xia, W., 2016. Autophagy induction by SIRT6 is involved in oxidative stress-induced neuronal damage. Protein Cell. 7(4), 281-290.

64. Lionaki, E., Markaki, M., Tavernarakis, N., 2013. Autophagy and ageing: insights from invertebrate model organisms. Ageing Res Rev. 12, 413-428.

Legends to figures

Fig. 1. Lysosomal activity and autophagic structures in metformin-treated protoscoleces. (A) Confocal imaging of Met-treated protoscoleces (1 mM) post-stained with acridine orange (AO). (a-b) Control protoscoleces. (c-d) Met-treated protoscoleces. Light field (a and c); fluorescence field (b and d). Bars: 200 µm. (B) Semi-quantitative estimation of acidic vesicular organelles (AVOs) with AO using Fluoroskan. Graph shows relative fluorescence levels between Met- or rapamycin (Rm)-treated protoscoleces in comparison with untreated control. Protoscoleces were exposed to supravital coloration with AO for a period of 30 min after treatment with 1 and 5 mM Met or 10 and 100 µM of rapamycin. In stained cells, the acidic compartments fluoresce bright red and the intensity of the fluorescence is proportional to the degree of acidity. Data are the mean ± S.D. of three independent experiments. *Statistically significant difference ($P < 0.05$) compared with control. (C) Transmission electron microscopy of control protoscoleces and treated with 1 mM Met for 4 days. (a-b) Control protoscoleces exhibiting intact parasite tissue. In (c-d), the damage induced by Met is shown. (c) Note the presence of autolysosomes (al) with degraded cytoplasmic content within them. (d) The presence of autophagosomes (a) and autolysosomes (al) was observed. ly, lysosomes; glc, glycogen deposits; g, glycocalyx; ld, lipid droplet; dc, distal cytoplasm; ve, vesicles; nu, nucleus. Bars indicate 1 µm.

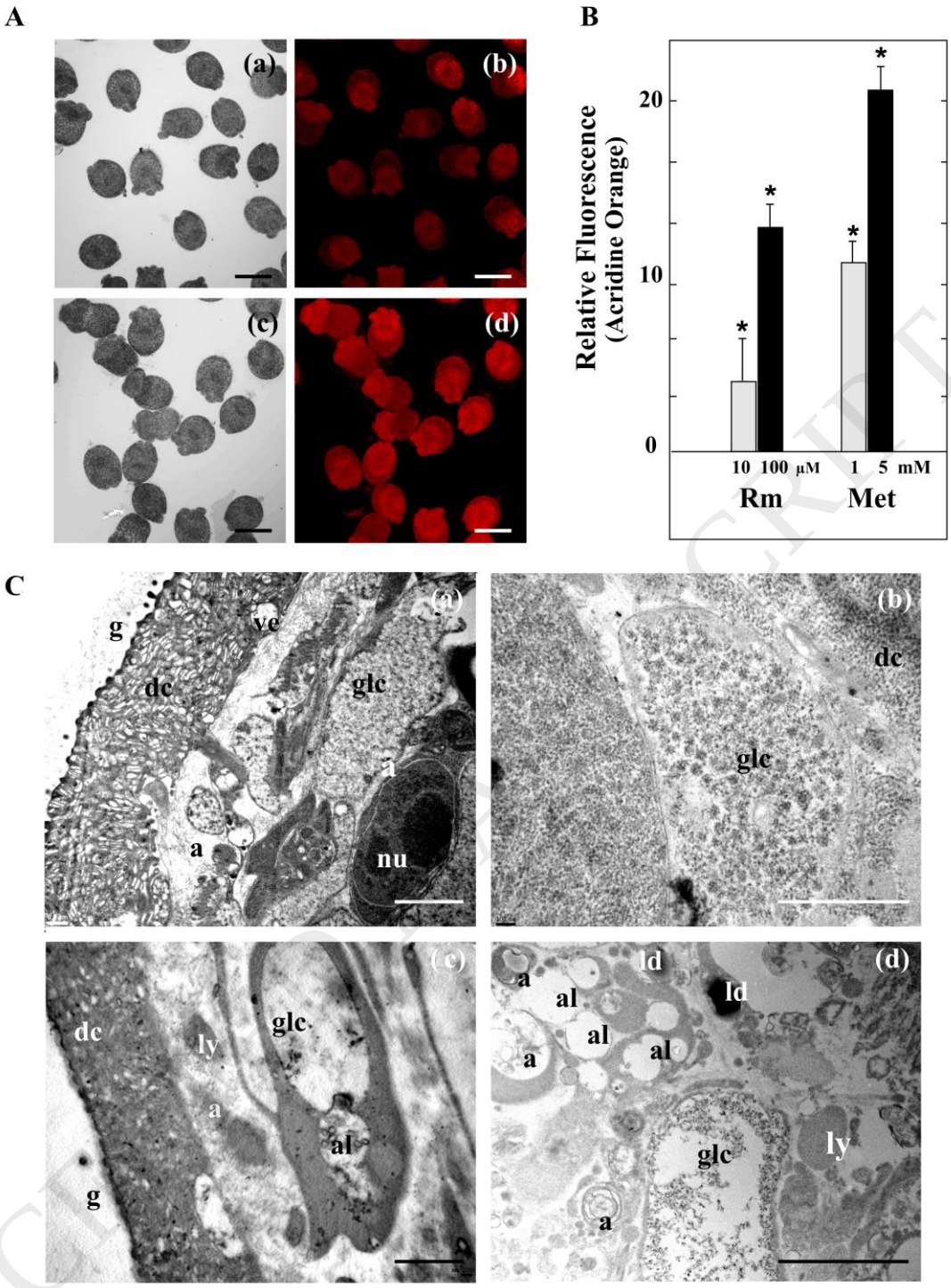

Fig. 2. Detection and immunolocalization of Eg-Atg8.1 from *E. granulosus* protoscoleces. (A) Immunoblot of Eg-Atg8.1 revealed with an antibody against human LC3. Total protein extracts from control (Co) and 10 mM Met-treated protoscoleces (Met) were loaded at 100 µg of total protein/lane. Both Eg-Atg8.1 and phosphatidylethanolamine-conjugated Eg-Atg8.1 (Eg-Atg8.1-PE) were detected. Polypeptide sizes are shown. (B) Confocal images of *in toto*

immunolocalization assays revealed with an antibody conjugated with Alexa 488 -green fluorescence- and counterstained with propidium iodide -red fluorescence-. Control (a-d) and Met-treated protoscoleces (e-h) incubated with anti-LC3 antibody. Inset images correspond to transmission microscopy. Tg: tegument; su: sucker; rc: rostellar cone; cc: calcareous corpuscle; tb: terminal bladder; arrowhead: Atg8.1-labelling around calcareous corpuscles. Bars indicate 50 μm.

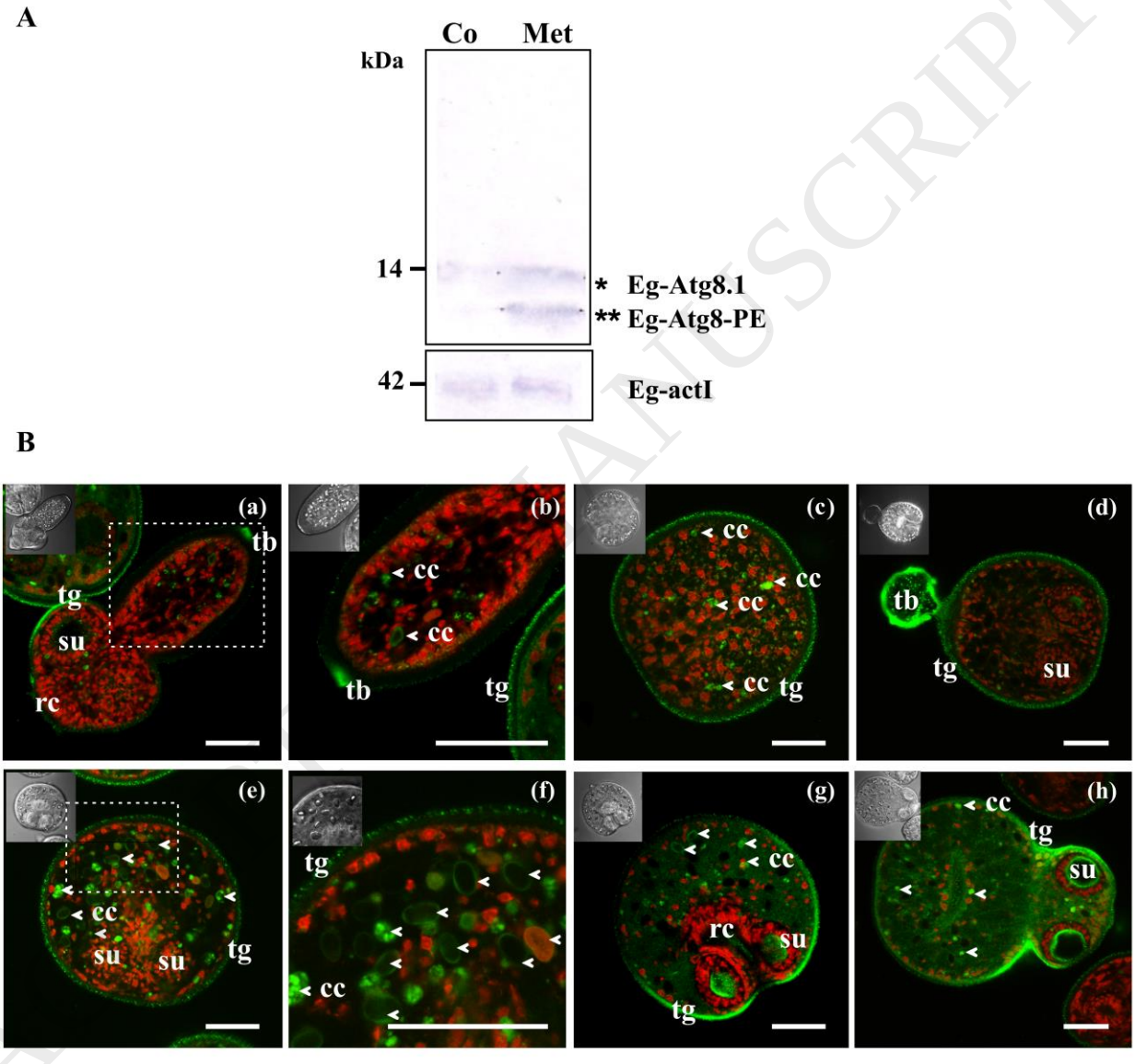

Fig. 3. Transcriptional changes of autophagy-related genes in metformin-treated larval stage. (A, C) Reverse Transcription (RT)-PCR analysis from total RNA of control (Co) or treated (Met) protoscoleces (PTS) and metacestodes (MTC). Amplification of Eg-actin I (*act*I) was used as a loading control. Molecular sizes of amplicons are indicated with arrowheads. Eg-*atg*:

autophagy-related gene. (B, D) Quantitative PCR analysis from total RNA of protoscoleces (PTS) and metacestodes (MTC) treated with Met compared to controls. Amplification of Eg-ezrin like protein (*elp*) was used as a reference gene. Fold change expression values are plotted. Data are the mean ± S.D. of three independent experiments. *Statistically significant difference ($P < 0.05$) compared with control.

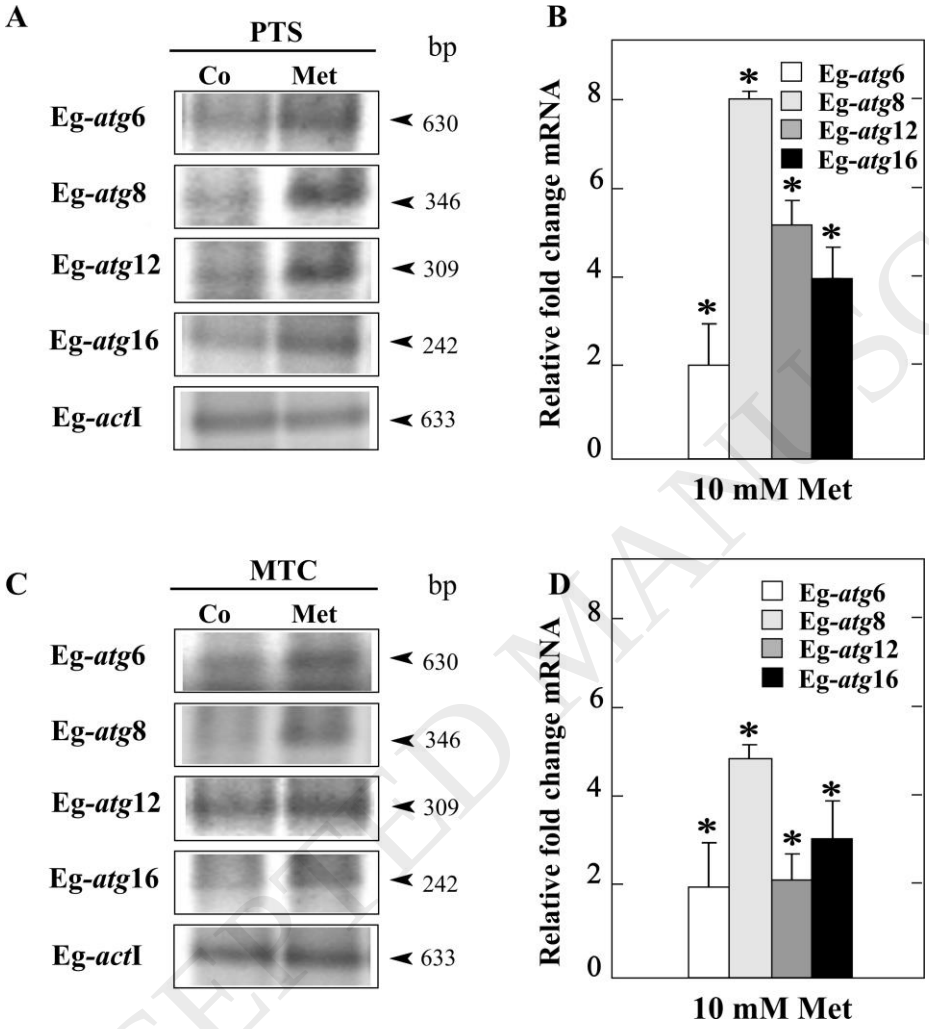

Fig. 4. Expression and immunolocalization of Eg-FoxO in metformin-treated protoscoleces. (A) Reverse Transcription (RT)-PCR analysis from total RNA of control (Co) or treated (Met) protoscoleces. Amplification of Eg-actin I (*act*I) was used as a loading control. Molecular sizes of amplicons are indicated with arrowheads. Eg-*foxO*: forkhead box O gene. (B) Quantitative PCR analysis from total RNA of control (Co) or treated (Met) protoscoleces. Amplification of Eg-ezrin like protein (*elp*) was used as a reference gene. Fold change expression values are plotted. Data are the mean ± S.D. of three independent experiments. *Statistically significant

difference ($P < 0.05$) compared with control. (C) Immunoblot of a phosphorylated (Eg-FoxO-P) and an acetylated (Eg-FoxO-Ac) form of Eg-FoxO revealed with an antibody directed against the posttranslationally modified form of human FoxO3 and FoxO1, respectively. Total protein extracts from control (Co) and 10 mM Met-treated protoscoleces (Met) were loaded at 100 μg of total protein/lane. Both Eg-FoxO-P and Eg-FoxO-Ac were detected. Polypeptide sizes are shown. (D) Partial amino acid sequence comparison between *Echinococcus* FoxO and human orthologs. Consensus (last line), total (uppercase letter), partial (lowercase letter), conservative changes (numeral), absence of consensus (dots) and gaps (dashes). GenBank accession numbers are: Hs-FoxO3, *Homo sapiens* FoxO3 (**NP_001446**); Hs-FoxO1, *H. sapiens* FoxO1 (**NP_002006**). Eg-FoxO, *E. granulosus* FoxO (**CDS21384**). (E) Subcellular immunolocalization of an acetylated (Eg-FoxO-Ac) and a phosphorylated (Eg-FoxO-P) form of Eg-FoxO in control (Co) and treated (Met) protoscoleces. Images of protoscoleces visualized by light transmitted microscopy (first and third column) and by fluorescence confocal microscopy obtained by overlapping the propidium iodide staining (red fluorescence) with the label of the antibody conjugated with Alexa 488 (green fluorescence, second and last column). The punctate staining for Eg-FoxO-Ac expression was evenly detected in both nucleus and cytoplasm. Nuclear expression is observed in yellow/orange, corresponding to the merged fluorescences. Boxed areas in (a) and (c) are shown in high magnification images in (c) and (g), respectively. tg: tegument; su: sucker; rc: rostellar cone; cc: calcareous corpuscle; tb: terminal bladder. Bars indicate 50 μm. (F) Semi-quantitative estimation of the acetylated Eg-FoxO form expression and its localization. Graph shows relative fluorescence levels between nuclear and cytoplasmic acetylated Eg-FoxO form expression from five photographs of Met-treated and control protoscoleces as shown in (D).